Δελτίο της Ελληνικής Γεωλογικής Εταιρίας, τομ. XLVII , 2013
Πρακτικά 13ου Διεθνούς Συνεδρίου, Χανιά, Σεπτ. 2013

Bulletin of the Geological Society of Greece, vol. XLVII 2013
Proceedings of the 13th International Congress, Chania, Sept. 2013

EARTHQUAKE CLUSTERS IN NW PELOPONNESE

Mesimeri M.[1], Papadimitriou E.[1], Karakostas V.[1] and Tsaklidis G.[2]

[1] *Aristotle University of Thessaloniki, Geophysics Department, mmesimer@geo.auth.gr, ritsa@geo.auth.gr,vkarak@geo.auth.gr.*

[2] *AristotleUniveristy of Thessaloniki, Department of Statistics and Operational Research, tsaklidi@math.auth.gr*

Abstract

Clusters commonly occur as main shock – aftershock (MS-AS) sequences but also as earthquake swarms, which are empirically defined as an increase in seismicity rate above the background rate without a clear main shock. A delcustering algorithm is employed to identify clusters from a complete catalog of earthquakes that occurred in the area of NW Peloponnese (Greece) during 1980-2007. In order to distinguish these clusters we calculate the skewness and kurtosis of seismic moment release for each cluster, since swarm-like sequences generally have lower skew value of moment release history than MS-AS. The spatial distribution of b-value was calculated for the entire catalog as for the declustered one, in order to correlate them with seismicity behavior of the region. Finally, the pre-stress field of Achaia 2008 earthquake was calculated aiming to associate the stress accumulation with the occurrence of the identified clusters.
Key words: *earthquake swarms, static stress changes, statistical seismology*

Περίληψη

Οι σεισμικές συγκεντρώσεις εκδηλώνονται ως ακολουθίες του τύπου κύριος σεισμός – μετασεισμοί αλλά και ως σμηνοσειρές, οι οποίες ορίζονται ως απότομες μεταβολές της σεισμικότητας χωρίς να κυριαρχεί κάποιος σεισμός σε μέγεθος. Εφαρμόστηκε αλγόριθμος με σκοπό την αναγνώριση των σεισμικών συγκεντρώσεων από ένα πλήρη κατάλογο για την περιοχή της ΝΔ Πελοποννήσου κατά την περίοδο 1980-2007. Ένα χαρακτηριστικό των σμηνοσεισμών αποτελεί η χαμηλή τιμή της λοξότητας της σεισμικής ροπής ως προς το χρόνο. Με σκοπό την διάκριση των σεισμικών συγκεντρώσεων σε σμηνοσεισμούς και μετασεισμικές ακολουθίες υπολογίζονται οι τιμές της λοξότητας και της κύρτωσης της σεισμικής ροπής ως προς το χρόνο για κάθε σεισμική συγκέντρωση. Επιπλέον υπολογίστηκε η χωρική κατανομή της παραμέτρου b τόσο για τον πλήρη κατάλογο όσο και για τον κατάλογο που προσεγγίζει την κανονική σεισμικότητα της περιοχής. Τέλος, υπολογίστηκε η κατανομή των τάσεων πριν την γένεση του σεισμού της Αχαΐας του 2008 με σκοπό την συσχέτιση της φόρτισης της περιοχής με την εκδήλωση σεισμικών συγκεντρώσεων.
Λέξεις κλειδιά: *σμηνοσεισμοί, μεταβολές πεδίου τάσεων, στατιστική σεισμολογία*

1. Introduction

Clustering of earthquakes in space and time indicates that interaction between earthquakes is an important component of the seismic cycle. There are three different types of earthquake sequences: (i) a mainshock followed by a number of aftershocks of decreasing magnitude and frequency, (ii) a slow buildup of seismicity (foreshocks) leading to a type (i) sequence and (iii) a gradual increase and decay of seismicity in time without a distinct mainshock. Earthquake sequences (i) typically occur in homogeneous material with a uniform external stress. Sequences (ii) tend to occur in material that is heterogeneous to some degree, or a moderate fracture density, with a non-uniform external stress. Sequences (iii) or swarms, occur in material that is extremely heterogeneous, or have high fracture density, with very concentrated external stress (Mogi, 1963).

One case of earthquake clustering is the occurrence of 'earthquake swarms', which can be defined as an increase in seismicity rate that lacks a clear main shock (Mogi, 1963; Sykes, 1970; Hill, 1977). Seismic swarms occur in a variety of different environments and might have a diversity of origins. Several studies were conducted to identify earthquake clusters and their spatiotemporal properties (Vidale and Shearer, 2006; Farell et al., 2009; Roland and McGuire, 2009; Holtkamp et al., 2011, among others).

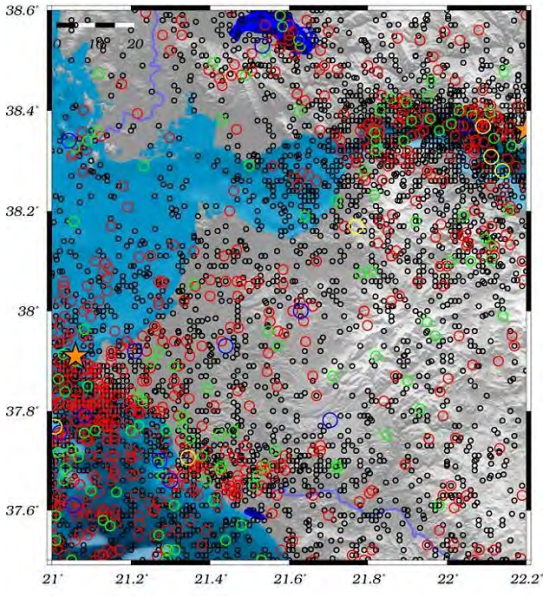

Figure 1 - Seismicity map of the complete catalogue (Mc ≥ 3.5) for the region of NW Peloponnese (1980-2007). Earthquakes with 3.5 ≤ M<6.0 are denoted by circles increasing in size according to the magnitude and M ≥ 6.0 are denoted by stars.

NW Peloponnese (Figure 1), which was selected as our target area, has experienced several moderate earthquakes in the last decades. In addition, several seismic sequences were recorded without a main shock with clearly discriminative magnitude. In the present work an effort is made for identifying earthquake clusters of both types that occurred in the region in the last decades and to investigate their spatio-temporal distribution, aiming to associate their occurrence with certain seismicity patterns.

2. Methods

In order to identify earthquake clusters from an earthquake catalogue and define their spatiotemporal properties, the following methods were applied.

2.1. Swarm Identification

Various algorithms are available to detect foreshock, mainshock and aftershock sequences (Reasenberg, 1985; Zhuang et al., 2002, among others). In this study, Reasenberg's (1985) algorithm was used to identify clusters from a complete catalogue. After the performance of declustering algorithm, we extract the catalogue that contains the clusters and we analyze them statistically (**see 2.3**) to distinguish swarm-like sequences from MS-AS. A swarm is defined if the following criteria proposed by Mogi (1963) are met: i) the maximum of the daily number of events in the sequence (N) is greater than twice the square root of the swarm duration in days (T): $N>2\sqrt{T}$ and ii) the total number of earthquakes in a sequence is at least 10 .

2.2. Calculating b-values

The b-value is a measure of the relative number of small to large earthquakes that occur in a given area and in a given time interval. In particular, the b-value is the slope of the frequency-magnitude distribution (Ishimoto and Iida, 1939; Gutenberg and Richter, 1944) for a given population of earthquakes. Studies have shown that the b-value changes with material heterogeneity (Mogi, 1962), thermal gradient (Warren and Latham, 1970), and applied stress (Scholz, 1968; Wyss, 1973; Urbancic et al., 1992; Schorlemmer et al., 2004; Schorlemmer and Wiemer, 2005; Schorlemmer et al., 2005).

The b-values determined in this study were calculated using the Zmap algorithm (Wiemer, 2001). Maximum-likelihood b-values were computed using equation 1 (Utsu, 1965; Aki, 1965; Bender, 1983):

Equation 1- b value calculation

$$b = \frac{1}{\bar{M} - M_{\min}} \log e$$

where $\bar{M}$ is the mean and M_{min} the minimum magnitude, respectively, of the given sample.

To examine how reliable our estimations are, a standard deviation δb of the b-value is estimated from the equation first derived by Aki (1965), or the improved formulation (eq. 2) by Shi and Bolt (1982):

Equation 2- error in b-value calculation

$$\delta b = 2.3 b^2 \sqrt{\frac{\sum_i (M_i - (M))^2}{n(n-1)}}$$

where n is the sample size.

2.3 Skewness and Kurtosis

Seismic swarms are distinguished from typical MS-AS by their unique seismicity patterns: the largest swarm events tend to occur later in the sequence, swarms contain several events as opposed to one clear mainshock, and swarm seismicity is more prolonged in time. One simple way to quantitatively identify earthquake clusters with swarm-like properties is through characterizing the timing of the largest event relative to the rest of the seismicity. To accomplish this, we calculate the skewness of moment release history and the kurtosis for each of the sequences that we analyze (Mesimeri, 2013). As described by Roland and McGuire (2009), a larger positive value of skewness is observed for pure aftershock sequences (approximately 30) while a lower or even negative value is observed for swarms (between -2 to 2). In addition, a large value of kurtosis is expected for MS-AS (kurtosis≥3) and a lower one for swarm-like sequences (kurtosis≤3) by the definition of kurtosis.

As proposed by Chen and Shearer (2011), for each swarm we normalize the time for each event since the beginning of the sequence by the mean time delay,

Equation 3- Mean time delay

$$t_i = \frac{(T_i - T_o)}{mean(T_i - T_o)} \quad i = 1, N$$

.

Next we consider the normalized timing of the largest event in the sequence t_{max}. Chen and Shearer (2011) classify clusters with $t_{max} \leq 0.4$ as early M_{max} (more similar to MS-AS) and clusters with $t_{max} \geq 0.4$ as late M_{max} (more swarm like) but in our study we consider $t_{max} \leq 0.3$ and $t_{max} \geq 0.3$ for MS-AS and swarm-like sequences, respectively. We use the skewness of moment release history

Equation 4-Skewness of moment release history

$$F(t) = \int_{t_0}^{t} M_o \, dt$$

to further quantify the difference between early M_{max} and late M_{max} clusters. For each event, the moment is estimated from the catalog magnitude (Hanks and Kanamori, 1979):

Equation 5

$$M_o(i) = 10^{1.5ML\,(i)+16.1},$$

where M_L is the local magnitude for each earthquake.

The centroid time of moment release is obtained from the weighted mean time (Jordan ,1991):

Equation 6- Centroid time

$$\bar{t} = \frac{\sum_1^N t_i \cdot M_o(i)}{\sum_1^N M_o(I)}$$

.

Individual moments (M_o) are normalized by

Equation 7

$$m_o(i) = \frac{M_o(i)}{\sum_1^N M_o(I)}$$

so that $F(t \rightarrow \infty) = 1$. The third ($\mu_3$) and the fourth ($\mu_4$) central moment of this sequence are

Equation 8-Third central moment

$$\mu_3 = \sum_1^N \left([\![ti - \bar{t}]\!] \right)^3 m_o(i) \,,$$

Equation 9 – Fourth central moment

$$\mu_4 = \sum_1^N \left([\![ti - \bar{t}]\!] \right)^4 m_o(i)$$

and the standard deviation:

Equation 10 –Standard deviation

$$\sigma = \sqrt{\sum_1^N \overline{ti - (t)}^2 \, m_o(i)}$$

.

The skewness and the kurtosis of moment release of each sequence are

Equation 11-Skewness

$$skewness = \mu_3/\sigma^3 \,,$$

Equation 12-Kurtosis

$$kurtosis = \mu_4/\sigma^4 \,.$$

2.4 Prestress Field Changes Calculations

In the pre-seismic stage, the main fault is locked and background seismicity is distributed in the surrounding area across small faults due to the raise of the stress level. King and Bowman (2003) have shown that a strong earthquake occurs when the distribution of the Coulomb stress around the fault has a certain pattern capable to trigger this rupture. This pattern depends on the geometry and kinematics of the ensuing rupture.

In the present study, Coulomb stress changes were calculated with the sense of slip opposite to the observed slip of the 2008 Achaia mainshock, according to the back-slip model suggested by Bowman and King (2001). This approach is based on the idea that before a strong earthquake the stress must accumulate not only on the fault itself, but also to a large region surrounding the fault prior to its failure. For the identification of this region, calculation of the stress field required for moving the causative fault with the orientation, displacement, and rake observed in the main shock is needed (Karakostas, 2009).

2.5 Data

The data used for the current study are taken from the monthly bulletins of the Geophysics Department of the Aristotle University of Thessaloniki (AUTH) and the Institute of Geodynamics of the National Observatory of Athens (NOA). The latitude and longitude appears with 3 digits in the AUTH dataset and with 2 digits in the NOA dataset. We did not proceed to any modifications since the error is larger than the accuracy of our data and the result is not affected. For the compilation of these bulletins, the recordings of the Hellenic Unified Seismographic Network (HUSN), maintained by the above Institutions as well as by Department of Geophysics of the University of Athens and the Laboratory of Seismology of the University of Patras were used. The catalogue that covers the time from 01/01/1980 to 31/12/2007, was checked for completeness and a threshold magnitude was identified.

3. Results

3.1 Clusters and their Statistical Properties

Wiemer and Wyss (2000) suggest that a careful estimate of the spatial and temporal homogeneity of the completeness magnitude (M_c) is required before deviations from a power law behavior for small magnitudes can be made. We employed the maximum curvature method and the M_c was found to be equal to M_c=3.5 for the entire period. We also calculate M_c for shorter time intervals (1980-1990, 1990-2007, 2000-2007) in which M_c remained unaltered.

The complete catalogue was declustered dividing the catalogue in 3 datasets, (i) the entire complete catalog, (ii) the one that contains only the clusters (1,383 events) and (iii) the declustered catalog (3262 events). The seismicity rate for the 3 datasets is shown in Figure 2 along with the events with magnitude M≥5.0, denoted by stars on the curve which contains the entire catalogue. From a visual inspection, we can recognize if the increase of the seismicity is due to a strong event or not.

The catalogue that contains the clustered events was thoroughly examined in order to more strictly define clusters and then distinguish MS-AS from earthquake swarms. From the initially 1,383 clustered events, 632 are kept that are distributed into 18 potential clusters. The spatial distribution of these clusters is shown in Figure 3, where the mean geographical coordinates of each cluster were plotted by stars. Additional information on the clusters properties such as starting time, duration and mean epicenter, is given in Table 1. For now on we will refer to each cluster by the code number given in Table 1.

In order to separate the swarm-like sequences from the MS-AS we calculate the skewness and the kurtosis of the seismic moment release for each event (Table 1). The t_{max} were also calculated for

this discrimination. If t_{max} is greater than 0.3 we have a swarm-like sequence and if t_{max} is lower than 0.3 is MS-AS or a swarm like sequence with an early main event, as mentioned above.

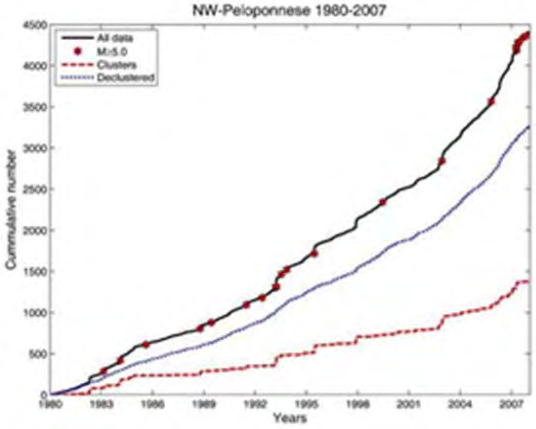

Figure 2 – Seismicity rates for the three data sets. Solid, dotted and dashed lines correspond to complete, declustered and clusters catalogues, respectively. Stars denote events with M≥5.0.

In Figure 4 the value of skewness of each cluster is plotted against to the value of kurtosis. For our data, it seems that clusters with skewness <2 and kurtosis<5 can be characterized as swarms, while clusters with skewness>2 and kurtosis>5 are MS-AS. Considering the value of t_{max} we conclude that clusters 03, 04, 07, 08, 10, 12, 18 are of MS-AS type, clusters 01, 02, 13-16 are swarms and clusters 05, 06, 09, 11, 17 are swarm like sequences with an early main event (t_{max} approximately zero).

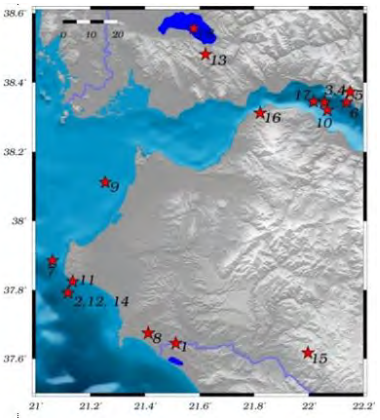

Figure 3 – Spatial distribution of earthquake clusters centres (denoted by star) for 1980-2007. The numbers are referring to Table 1

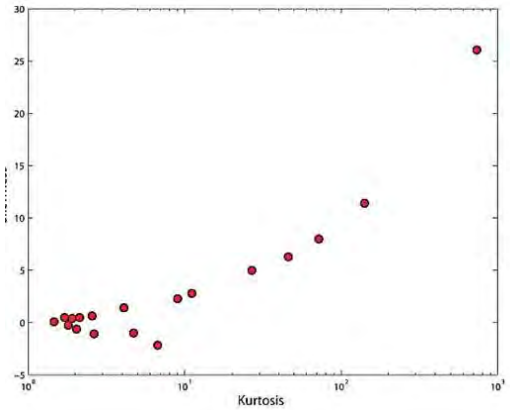

Figure 4 –Calculated skewness of seismic moment release plotted against the kurtosis of each cluster

3.2 b-value Distribution

In Figure 5 the b-value spatial distribution of the complete (Figure 5a) and the declustered (Figure 5b) catalogue is shown, as been calculated by Zmap, along with earthquakes epicentral distribution. Calculations were performed on the nodes of a normal grid superimposed on the study area. A constant 15km radius was chosen to calculate b-values, compromising maximum coverage and details in b-values spatial variation. The number of events with $M \geq M_c$ are set to 25 and the grid selection is 0.01^o x 0.01^o. In addition, two more limitations are applied to get reliable results. Firstly we consider only values estimated from datasets with magnitude range $\Delta M \geq 1.0$, where ΔM is the difference between M_{max} and M_c of each bin, and finally we choose b-values with $\delta b < 0.4$.

Table 1 - Basic properties of the clusters shown by asterisks in map of Figure 3. The two last columns correspond to the statistical parameters skewness and kurtosis, respectively

S/N	Starting Time	Days	M_{max}	# of events	Lon. (°E)	Lat. (°N)	T_{max}	Sw	K
1	1982/04/23,02:24	14.8	4.8	57	21.513	37.645	0.4	0.4	1.7
2	1983/03/13,13:48	4.2	4.3	13	21.119	37.792	1.1	-1.0	4.7
3	1984/01/02,07:07	5.3	4.5	14	22.023	38.346	0.0	2.27	9.01
4	1984/02/11.05:04	6.9	5.6	37	22.064	38.351	0.08	11.4	141
5	1984/11/09,09:51	0.7	3.9	10	22.151	38.373	0	0.3	1.9
6	1984/11/20,19:30	10.7	3.7	13	22.133	38.340	0	-0.6	2.0
7	1988/10/16,12:34	16.3	6	27	21.062	37.885	0	7.9	71.9
8	1993/03/26,11:45	8.4	5.4	86	21.413	37.675	0	2.7	11.1
9	1994/10/13,12:40	12.2	4	13	21.255	38.112	0.1	0.4	2.1
10	1995/06/15,00:15	24.8	6.5	82	22.068	38.320	0	26.0	735
11	2002/09/14,19:46	16.04	4.6	35	21.128	37.823	0	1.4	4.1
12	2002/12/02,04:58	23.03	5.4	47	21.115	37.795	0	6.28	46.0
13	2012/12/29,22:22	2.5	4.2	12	21.662	38.481	1.35	-1.0	2.6
14	2003/01/04,20:00	18.88	4.7	26	21.126	37.795	0.07	-0.2	1.8
15	2005/01/26,05:46	0.55	4.5	4	21.997	37.617	1.16	-2.1	6.73
16	2005/10/17,22:15	4.02	4.0	22	21.822	38.321	0.3	0.07	1.46
17	2007/01/07,14:47	13.94	4.3	60	22.018	38.341	0	0.63	2.55
18	2007/04/09,05:02	5.88	5.3	66	21.579	38.556	0.67	4.98	26.8

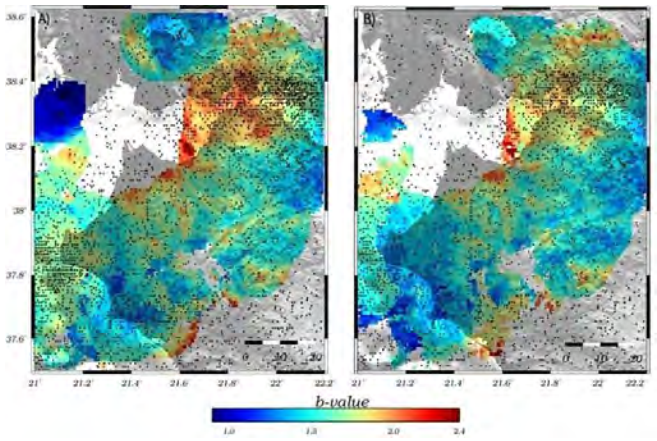

Figure 5 – b-value distribution a) for the complete catalogue and b) for the declustered catalogue (1980-2007). Bright and dark zones indicate high and low b-values, respectively.

In order to associate the b-value with the seismicity of the region we use both the entire catalogue and the declustered one. It is pictured (Figure 5) that regions with high seismicity, such as the western part of Corinth Rift, exhibit high b-values both in the declustered and the entire catalogue. For the regions that experience low seismicity, a b-value was not possible to be calculated.

3.3 Coulomb Stress Changes

In order to examine the relation between the spatial appearance of clusters and the pre-stress field of Achaia 2008 earthquake, we adopted the GCMT fault plane solutions for the strongest event in each cluster with a main event of M≥5.0 (Table 2).The pre-stress field was calculated inverting the sense of slip on the fault of 2008 earthquake according to the faulting type of the main event of each cluster (Figure 6). In these figures, dark regions denote negative changes in ΔCFF and inferred decrease likelihood of fault rupture. These regions are called stress shadows (Harris and Simpson 1993, 1996). Bright regions represent positive ΔCFF and increased likelihood of fault plane rupture. Most of the clusters were in the areas of high stress concentration (bright zones) with only the exception of cluster 8.

Table 2 – Information on the source parameters of M≥5.0 earthquakes that occurred in NW Peloponnese during 1980-2008 Fault plane solutions are taken from GCMT catalogue.

Origin Time	Epicenter		Mw	Mechanism			Depth	Event
	Lon.	Lat.		Strike	Dip	Rake		
1984/02/11,08:02	22.09	38.36	5.6	77	28	-121	15	4
1988/10/16,18:40	20.9	37.95	5.8	301	76	-3	29	7
1993/03/26,11:58	21.3	37.66	5.4	30	86	150	15	8
1995/06/15,00:15	22.2	38.36	6.5	265	43	-103	15	10
2002/12/02,04:59	21.08	37.79	5.6	36	56	-160	15	12
2007/04/10,03:17	21.63	38.55	5.0	320	41	-69	13.9	18
2008/06/08,12:25	21.53	37.95	6.5	208	88	178	24.7	Achaia

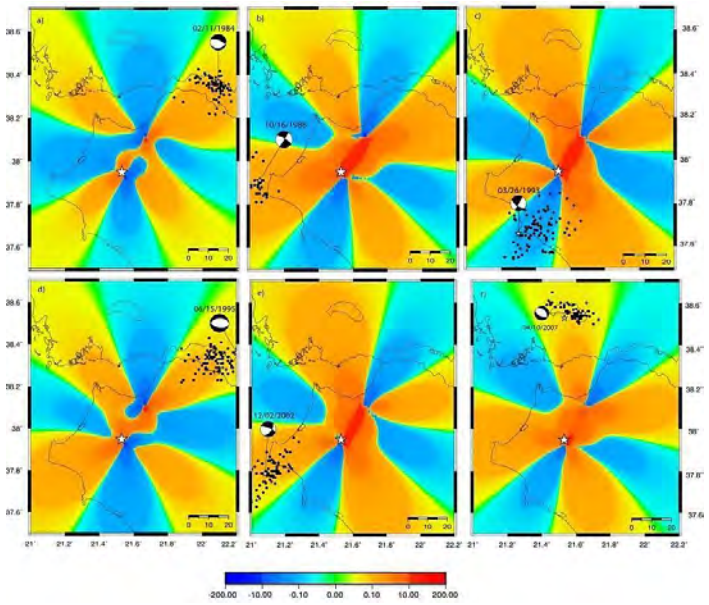

Figure 6 – Stress field modelled by reversing the sense of slip observed in Achaia 2008 earthquake (M=6.4) for the fault plane solution of events in Table 2. Dots represent the epicenters of each cluster, the big star depicts the epicentre of Achaia 2008 earthquake. In a) is cluster 4, b) cluster 7, c) cluster 8, d) cluster 10 (Aigio earthquake), e) cluster 12 and f) cluster 18.

4. Discussion – Conclusions

For the period 1980-2007 18 clusters were identified in the area of NW Peloponnese, with the employment of a declustering algorithm in a complete earthquake catalogue. Clusters were divided into three types (MS-AS, swarms and swarm-like sequences) according to their history of seismic moment release (skewness and kurtosis) and the occurrence time of the main event. Spatial distribution of calculated b-values on a normal grid superimposed on the study area reveals that high b-values are in areas that experience high seismicity. The stress associated with the preparation procedures of 2008 Achaia main shock (M=6.4) is in agreement with the 5 major clusters, as those are placed in the red lobes, indicating that the stress was accumulated in the region around the fault and swarm-like activity was encouraged.

5. Acknowledgments

The GMT system (Wessel and Smith, 1998) was used to plot the figures and the Zmap software (Wiemer, 2001) for the b-value calculations. The stress tensors were calculated using a program written by J. Deng (Deng and Sykes, 1997) who used the DIS3D code of S. Dunbar and Erikson (1986) and the expressions of G. Converse. The paper is benefitted by the thorough revision of Antonis Vafidis and an anonymous reviewer. This work was supported in part by the THALES Program of the Ministry of Education of Greece and the European Union in the framework of the project entitled "Integrated understanding of Seismicity, using innovative Methodologies of Fracture mechanics along with Earthquake and non extensive statistical physics – Application to the geodynamic system of the Hellenic Arc, SEISMO FEAR HELLARC". Geophysics Department Contibution 812.

6. References

Aki K. 1965. Maximum likelihood estimate of b in the formula log N=a−bM and its confidence limits, *Bull. Earthq. Res. Inst. Univ. Tokyo,* 43, 237–239.

Bender B. 1983. Maximum likelihood estimation of b values for magnitude grouped data, *Bull. Seismol. Soc. Am.*, 73, 831–851.

Bowman D. and King G. 2001. Accelerating seismicity and stress accumulation before large earthquakes, *Geophys. Res. Lett.,* 28, 21, 4039-4042,DOI: 10.1029/2001GL013022.

Chen X. and Shearer P. 2011. Comprehensive analysis of earthquake source spectra and swarms in the Salton Trough, California, *J. Geophys. Res.*, 116, B09309, doi:10.1029/2011JB008263.

Deng J. and Sykes L. 1997. Evolution of the stress field in southern California and triggering of moderate-size earthquakes: A 200-year perspective*, J. Geophys. Res.*, 102, B5, 9859-9886, DOI: 10.1029/96JB03897.

Erikson L. 1986. User's Manual for DIS3D: A Three-Dimensional Dislocation Program with Applications to Faulting in The Earth, *Master's Thesis*, Stanford University, Stanford, CA, 167 pp.

Farrell J., Husen S. And Smith R. 2009. Earthquake swarm and b-value characterization of the Yellowstone volcano-tectonic system, *J. Volcanol. Geotherm. Res.*, 188, 260–276.

Gutenberg B. and Richter C.F. 1944. Frequency of earthquakes in California, *Bull. Seismol. Soc. Am.* 34, 185–188.

Hanks T. C. and Kanamori H. 1979. A moment magnitude scale, *J. Geophys. Res.,* 84, 2348-2350.

Harris R. and Simpson R. 1993. In the shadow of 1857:An evaluation of the static stress changes generated by the M8 Ft. Tejon, California, earthquake, *EOS Trans. Am. Geophys. Un.,* 74, 427.

Harris R. and Simpson R. 1996. In the shadow of 1857: The effect of the great Ft. Tejon earthquake on subsequent earthquakes in southern California, *Geophys. Res. Lett.*, 23, 229–232.

Hill D. 1977. Model for earthquake swarms, *J. geophys. Res.*, 82, 1347–1352.

Holtkamp S., Pritchard M. and Lohman R. 2011. Earthquake swarms in South America, *Geophys. J. Int.*, 187, 128-146.

Jordan T. 1991. Far-field detection of slow precursors to fast seismic ruptures, *Geophys. Res. Lett.*,18, 2019-2022.

Ishimoto M. and Iida K. 1939. Observations of earthquakes registered with the microseismograph constructed recently, *Bull. Earthq. Res. Inst. Univ. Tokyo*, 17, 443–478.

Karakostas V. 2009. Seismicity patterns before strong earthquakes in Greece, *Acta Geophys.*, 57, 2, 367-386, DOI: 10.2478s11600-009-0004-y.

King G. and Bowman D. 2003. The evolution of regional seismicity between large earthquakes, *J. Geophys. Res.,* 108, B2, 2096, DOI: 10.1029/2001JB000783.

Mesimeri M. 2013. Spatio-temporal properties of earthquake swarms, *MSc thesis*, Aristotle University Thessaloniki, Thessaloniki, Greece, 84 pp (in Greek).

Mogi K. 1962. Magnitude–frequency relation for elastic shocks accompanying fractures of various materials and some related problems in earthquakes, *Bull. Earthq. Res. Inst. Univ. Tokyo,* 40, 831–853.

Mogi K. 1963. Some discussions on aftershocks, foreshocks and earthquake swarms—the fracture of a semi-infinite body caused by an inner stress origin and its relation to the earthquake phenomena, *Bull. Earthq. Res. Inst. Univ. Tokyo,* 41, 615–658.

Reasenberg P. 1985. Second-order moment of central California seismicity, 1969–1982, *J. Geophys. Res.*, 90, 5479–5495.

Roland E. and McGuire J. 2009. Earthquake swarms on transform faults, *Geophys. J. Int.*, 178, 1677–1690.

Scholz C. 1968. The frequency–magnitude relation of microfracturing in rock and its relation to earthquakes, *Bull. Seismol. Soc. Am.,* 58, 399–415.

Schorlemmer D., Weimer S. and Wyss M. 2004. Earthquake statistics at Parkfield: 1.Stationarity of b values, *J. Geophys. Res.,* 109, B12307. doi:10.1029/2004JB003234.

Schorlemmer D. and Wiemer S. 2005. Microseismicity data forecast rupture area, *Nature,* 434, 1086.

Schorlemmer D., Wiemer S. and Wyss M. 2005. Variations in earthquake-size distribution across different stress regimes, *Nature,* 437, 539–542.

Shi Y. and Bolt B. 1982. The standard error of the Magnitude-frequency b value, *Bull. Seism. Soc. Am.*, 72, 1677-1687.

Sykes L. 1970. Earthquake swarms and sea-floor spreading, *J. geophys.Res.,* 75, 6598–6611.

Utsu T. 1965. A method for determining the value of b in a formula log N=a−bM showing the magnitude frequency for earthquakes, *Geophys. Bull. Hokkaido Univ.*, 13, 99–103.

Urbancic T., Trifu C., Long J. and Toung R. 1992. Space–time correlations of b values with stress release, *Pure Appl. Geophys.,* 139, 449–462.

Vidale J. and Shearer P. 2006. A survey of 71 earthquake bursts across southern California: Exploring the role of pore fluid pressure fluctuations and aseismic slip as drivers, *J. Geophys. Res.*, 111, B05312, doi:10.1029/2005JB004034.

Warren N. and Latham G. 1970. An experimental study of thermally induced microfracturing and its relation to volcanic seismicity, *J. Geophys. Res.*, 75, 4455-4464.

Wessel P. and Smith W. 1998. New, improved version of the generic mapping tools released, *EOS Trans. AGU,* 79, 579.

Wiemer S. 2001. A software package to analyze seismicity: ZMAP, *Seism. Res. Lett.*, 72, 373-382.

Wiemer S. and Wyss M. 2000. Minimum magnitude of completeness in earthquake catalogs: examples from Alaska, the western United States, and Japan, *Bull. Seismol.Soc. Am.*, 90, 859–869.

Wyss M. 1973. Towards a physical understanding of the earthquake frequency distribution, *Geophys, J. R. Astron. Soc.*, 31, 341-359.

Zhuang J., Ogata Y. and Vere-Jones D. 2002. Stochastic Declustering of Space-Time earthquake Occurrences, *Journal of the American Statistical Association*, 97, 458, 369-380.